Solar Irradiance from 165 to 400 nm in 2008 and UV Variations in Three Spectral Bands During Solar Cycle 24

Mustapha Meftah, David Bolsée, Luc Damé, Alain Hauchecorne, Nuno Pereira, Abdanour Irbah, Slimane Bekki, Gaël Cessateur, Thomas Foujols, Rémi Thiéblemont

Solar Physics
DOI: 10.1007/•••••-•••-•••-••••-•

Solar Irradiance from 165 to 400 nm in 2008 and UV variations in 3 spectral bands during Solar Cycle 24

M. Meftah[1] · **D. Bolsée**[2] · **L. Damé**[1] · **A. Hauchecorne**[1] · **N. Pereira**[2] · **A. Irbah**[1] · **S. Bekki**[1] · **G. Cessateur**[2] · **T. Foujols**[1] · **R. Thiéblemont**[1] ·

Abstract — Accurate measurements of solar spectral irradiance (SSI) and its temporal variations are of primary interest to better understand solar mechanisms, and the links between solar variability and Earth's atmosphere and climate. The *SOLar SPECtrum* (SOLSPEC) instrument of the *Solar Monitoring Observatory* (SOLAR) payload onboard the *International Space Station* (ISS) has been built to carry out SSI measurements from 165 to 3088 nm. We focus here on the ultraviolet (UV) part of the measured solar spectrum (wavelengths less than 400 nm) because the UV part is potentially important for understanding the solar forcing of Earth's atmosphere and climate. We present here SOLAR/SOLSPEC UV data obtained since 2008, and their variations in three spectral bands during Solar Cycle 24. They are compared with previously reported UV measurements and model reconstructions, and differences are discussed.

Keywords: Solar Irradiance; Solar Cycle; Instrumentation and Data Management; Instrumental Effects

1. Introduction

The solar spectrum is a key input for different disciplines such as:

- Solar Physics where the solar spectrum characterizes the activity of the Sun's outer layers (photosphere, chromosphere, and corona). By comparison with the theoretical reconstructions, an accurately measured solar spectrum allows to validate temperature, composition, and densities of the solar atmosphere.

[1] Université Paris Saclay, Université Paris VI - Pierre et Marie Curie, CNRS/INSU, LATMOS-IPSL, 11 Boulevard d'Alembert, 78280 Guyancourt, France
Email: Mustapha.Meftah@latmos.ipsl.fr
[2] Belgian Institute for Space Aeronomy (BIRA-IASB), Ringlaan 3, B-1180 Brussels, Belgium
Email: David.Bolsee@aeronomie.be

- Climate Physics where solar-dependent processes are recognized as major drivers of rapid climate changes. Climate models require time-varying solar spectra as forcing. The available information is often based on solar reconstructions and models. However, it is not clear that they correctly represent the different levels of solar activity, notably ultraviolet (UV) levels. As a reminder, atmospheric models with representation of the middle stratosphere have been developed (Hegglin *et al.*, 2010). They strongly focus on simulating ozone, stratospheric dynamics (Strahan *et al.*, 2011), and testing knowledge of what controls global ozone (Oman *et al.*, 2010), notably the springtime polar ozone depletion (von Hobe *et al.*, 2013). The acknowledgement that the atmosphere at its different altitude ranges needs to be modeled as a coupled entity is relatively recent. Currently weather forecast models are including a representation of the mesosphere as it enhances the long term predictability power of the model. Solar variability forces the atmosphere at different altitudes by different mechanisms. The signal is amplified at the upper layers showing some degree of linearity in the chemistry. However, the signal becomes smaller and more complex at lower altitudes making it difficult to extract from model natural variability. Furthermore, atmosphere numerical models seem sensitive to the choice of solar irradiance variability used to force the model. As example, solar spectral irradiance (SSI) measurements in the Herzberg continuum will help to address several questions concerning the climate response to variable solar forcing (Sukhodolov *et al.*, 2016). About the stratospheric ozone, the total column ozone data records analysis show a clear 11-year signature, compatible with the Solar Cycle. However, models have so far not been able to reproduce completely the profile and magnitude of the signal (Austin *et al.*, 2008). In fact, many meteorological quantities are correlated with the 11-year solar signal but what are the mechanisms behind those signals?

Before 1970, very few reliable solar irradiance measurements above the atmosphere are available. There is the Neckel and Labs solar spectrum (Labs and Neckel, 1968; Neckel and Labs, 1981; Neckel and Labs, 1984), which is a reference spectrum obtained from ground-based and high-altitude measurements. From 1978, regular space-based measurements of the solar irradiance started. These space-based measurements began with the Shuttle borne Solar Backscatter UltraViolet spectrometer (Cebula, Hilsenrath, and Guenther, 1989; Cebula, DeLand, and Hilsenrath, 1998). The first regular space-based monitoring of the solar spectrum over a broad range (240–2380 nm) was carried out by the *SCanning Imaging Absorption spectroMeter for Atmospheric CHartographY* (SCIAMACHY) onboard Environment Satellite (Bovensmann *et al.*, 1999; Pagaran, Weber, and Burrows, 2009; Pagaran *et al.*, 2011). An overview of the main satellite missions that have made SSI observations at wavelengths higher than 100 nm is given by Ermolli *et al.* (2013).

SOLAR/SOLSPEC is a space-based spectro-radiometer developed by CNRS-LATMOS (France), and by BIRA-IASB (Belgium) with a major collaboration of the Heidelberg Observatory (Germany). It is externally mounted on the Columbus module of the *International Space Station* (ISS). The instrument measures the solar spectral irradiance above the atmosphere since 2008

and is still operational today. SOLAR/SOLSPEC consists of three separated double-spectrometers that use concave holographic gratings made by Jobin-Yvon to cover the specific 'UV' (165–371 nm), 'VIS' (285–908 nm), and 'IR' (646–3088 nm) spectral ranges. The spectral resolution of the 'UV' spectrometer is ranging from 0.6 nm to 1.6 nm, whereas the 'VIS' spectrometer is ranging from 1.6 nm to 2.1 nm, and the 'IR' spectrometer is ranging from 7 nm to 9.5 nm. Using a mechanical shaft, all the gratings are rotating simultaneously and scanning the three spectral ranges at the same time. The detectors are Electro-Mechanical Research photo-multiplier (PM) tubes in the 'UV' and 'VIS' spectral ranges, and a Hamamatsu P2682 PbS cell cooled at -20^{o}C in the 'IR' spectral band. SOLAR/SOLSPEC scientific objectives, instrument performances, and absolute calibration using a blackbody as primary standard source are described in more details by Thuillier *et al.* (2009) and Bolsée (2012).

The present article is dedicated to the UV portion (165–400 nm) of the solar spectrum and its temporal variations during Solar Cycle 24. Measurements from two separated double-spectrometers of SOLAR/SOLSPEC ('UV' and 'VIS') are combined. From these data, we obtained the UV solar spectrum above the Earth's atmosphere at a distance of one astronomical unit (initial values for studying the UV solar variability). SOLAR/SOLSPEC measurements are compared with previously reported solar UV measurements and model reconstructions and differences are discussed. SOLAR/SOLSPEC UV spectra are first compared with the *ATmospheric Laboratory for Applications and Science* (ATLAS) composite (Thuillier *et al.*, 2003) and with the Solar Irradiance Reference Spectra (SIRS) for the 2008 Whole Heliosphere Interval (WHI) corresponding to the solar Carrington rotation 2068 from mid-March to mid-April 2008 (Woods *et al.*, 2009). Similarly, SOLAR/SOLSPEC UV spectra are compared with reconstructions issued from the Spectral And Total Irradiance REconstruction for the Satellite era (SATIRE-S) semi-empirical model (Yeo *et al.*, 2014).
Degradation of the SOLAR/SOLSPEC instrument is highlighted, providing information for the development of future space-based UV instruments.
Finally, we present SOLAR/SOLSPEC UV SSI temporal variations from 2010 to 2015 in three spectral bands (165–180, 180–200, and 200–242 nm).

2. SOLAR/SOLSPEC Observations and Corrections

SOLAR/SOLSPEC was exposed to sunlight for the first time on April 5, 2008. The duration to record a solar spectrum (165–3088 nm) is less than 17 minutes. Between April 2008 and May 2016, more than 700 solar spectra were acquired. The fundamental issues for solar spectra measurements are:

- High accuracy to determine a reference solar spectrum,
- And long-term stability to accurately determine SSI change with time.

A typical day of acquisition consists of one solar spectrum measurement and three calibrations for different purposes (radiometric calibrations, spectral resolutions, and wavelength scales). The deuterium lamp (nominal or spare) allows a calibration of the 'UV' spectral band. Similarly, the tungsten ribbon lamp

(nominal or spare) allows a calibration of the 'VIS' spectral band. Two tungsten ribbon lamps (nominal and redundant) are associated with the 'IR' spectral band. Moreover, a helium hollow cathode lamp controls spectral resolutions and wavelength scales for the 'UV' and the 'VIS' spectral ranges. Thus, SOLAR/SOLSPEC has on-board standards (*i.e.* a lamps system) for calibration to identify possible SSI long-term changes. Indeed, the lamps are used for checking the instrument stability with time in order to provide reference data for aging corrections. However, these corrections are not straightforward (degradation of the lamps themselves as shown in Figure 1, lamps power supply failure, *etc.*). For example, the calibration of the 'UV' spectral band (deuterium lamps) was no longer possible since April 2009 due to the power supply failure of the deuterium lamps.

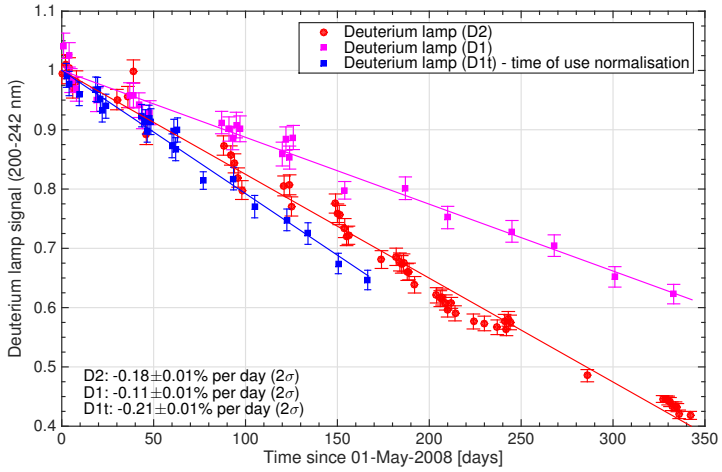

Figure 1. Temporal variations of SOLAR/SOLSPEC signal (200–242 nm) during calibrations with deuterium lamps (D1 and D2). The blue curve (D1t) represents the normalized temporal variation during a calibration with the D1 lamp for the same operation time as the D2 lamp.

Other calibrations allow to quantify the SOLAR/SOLSPEC quartz window transmission decreases. Indeed, the solar spectrum measurements are done with or without the quartz window in front of the entrance slit. The mechanical shutters and the quartz windows are used as a shield for limiting the degradation of the optical components due to the harsh space environment.

2.1. SOLAR/SOLSPEC Preflight Calibration and Expected Uncertainties

Pre-flight calibration to identify critical SOLAR/SOLSPEC performance parameters was described by Thuillier *et al.* (2009) and in more details in Bolsée (2012). Before the SOLAR mission, the first version of the SOLSPEC instrument has flown on SpaceLab I, on the ATLAS missions, and on EURECA. It provided data from 200 to 2400 nm (Thuillier *et al.*, 2003). This heritage has been taken into account in the design of SOLAR/SOLSPEC to increase its accuracy (Thuillier *et al.*, 2009). Pre-flight, the absolute calibration of SOLAR/SOLSPEC was

carried out using the spectral irradiance standards, such as the deuterium lamps and the blackbody of the *Physikalisch-Technische Bundesanstalt* (PTB, Braunschweig, Germany). During the absolute calibration at the PTB, the temperature of the SOLAR/SOLSPEC instrument was 23.3±1.5^{o}C.

Expected standard measurements uncertainties (1 σ) are between 2% to 4% in the 165–370 nm range and less than 2% in 370–400 nm (see Bolsée, 2012), which correspond to begin of life (BOL) values for SOLAR/SOLSPEC uniform temperatures (no temperature gradient).

2.2. SOLAR/SOLSPEC SSI Equation – Ideal Case

The SOLAR/SOLSPEC instrument has made continuous SSI measurements from April 2008 until today. In the best case (BOL and SOLAR/SOLSPEC temperature close to 23^{o}C), Equation 1 allows to determine the SSI evolution over time.

$$SSI_S(\lambda,t) = \left(S_n(\lambda,t) - \frac{< DC(t) >}{\tau(t)}\right) \times R(\lambda,t) \times \left(\frac{z(t)}{1\,au}\right)^2, \qquad (1)$$

where $SSI_S(\lambda,t)$ is the SSI as measured by SOLAR/SOLSPEC at a given wavelength (λ) and for a given time (t). $S_n(\lambda,t)$ (in counts s^{-1}) is the linearized signal provided by the detector (solar blind photomultiplier). The two spectral ranges ('UV' and 'VIS') are linear within their whole dynamical range (until 20 000 counts s^{-1}). $< DC(t) >$ (in counts) is the mean dark current of the detector taken before and after a solar spectrum measurement during the integration time (τ(t) in s). $R(\lambda,t)$ (in mW m^{-2} nm^{-1} counts^{-1} s) represents the absolute responsivity of the instrument. $z(t)$ (in km) is the distance between SOLAR/SOLSPEC and the Sun. The astronomical unit (1 au) is equal to 149 597 870.700 km.
The first SOLAR/SOLSPEC UV spectral distribution of the Sun's radiation at the mean Earth-Sun distance of one astronomical unit is shown in Figure 2 (red curve). No correction was applied such as photocathode quantum efficiency change with the temperature, which is a relatively weak effect. All solar spectra acquired between April 2008 and August 2015 are shown in blue for the 'UV' spectral band and in green for the 'VIS' spectral band. One can notice than the SOLAR/SOLSPEC SSI variations are much higher than the expected values. Indeed, below 400 nm, the long-term SSI variability increases with decreasing wavelength, reaching ∼15% of SSI variation at 165 nm using SATIRE-S data from 2008 to 2015. Yet, the SOLAR/SOLSPEC SSI variation at 165 nm can reach more than 80% from 2008 to 2015. This is obviously an abnormal variation, which highlights the degradation of the SOLAR/SOLSPEC instrument. Indeed, SOLAR/SOLSPEC such as different solar space-based instruments (Meftah *et al.*, 2014a; Cessateur *et al.*, 2016) is vulnerable to the degradation due to the space environment (BenMoussa *et al.*, 2013). Thus, the SOLAR/SOLSPEC signal ($S_n(\lambda,t)$) may evolve over time. Moreover, possible mechanical distortions (location of intermediate and exit slits) associated with temperature gradients can change the responsivity of the instrument.

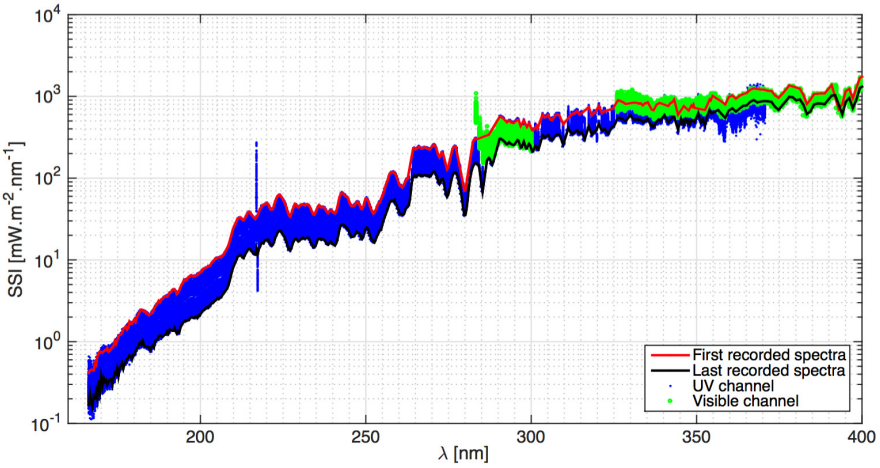

Figure 2. Measured spectral distribution of UV SSI (165–400 nm) from April 2008 to August 2015. Measurements of the 'UV' spectral band are represented with the blue dots. Measurements of the 'VIS' spectral band are represented with the green dots. The red curve represents the first SOLAR/SOLSPEC UV spectrum. The black curve represents the last UV solar spectrum obtained in August 2015.

2.3. SOLAR/SOLSPEC SSI Equation – Real Case

With the main correction factors, Equation 2 allows to determine a more realistic SOLAR/SOLSPEC SSI evolution over time.

$$SSI_R(\lambda,t) = SSI_S(\lambda,t) \times \frac{1}{1-\frac{\alpha_T(\lambda,t)}{100}\times(T_P - T_S(t))} \times \frac{1}{Deg(\lambda,t)} \times \frac{1}{I_E(\lambda,t)}, \quad (2)$$

where $\alpha_T(\lambda,t)$ is the temperature coefficient of the UV PM ($\%\,^oC^{-1}$). T_P represents the temperature reference of the UV PM during ground calibration (23.3^oC). $T_S(t)$ (in ^oC) represents the temperature of the UV PM in space. $Deg(\lambda,t)$ characterizes the degradation of the instrument (dimensionless factor where $Deg(\lambda,t) \leqslant 1$). The SOLAR/SOLSPEC internal optics and the quartz plate degradations can be monitored. Correction of the absolute responsivity ($R(\lambda,t)$) degradation of the instrument could have been obtained with the deuterium lamps calibration during a period. $I_E(\lambda,t)$ corresponds to instrumental effects that impact the optical quality of the instrument. $I_E(\lambda,t)$ is a dimensionless factor, which is equal to 1 for an optimal calibration of the instrument at a temperature of 23.3^oC such as the absolute calibration at the PTB.

2.4. Reversible Instrumental Effects Mainly Depicted by the $I_E(\lambda,t)$ Dimensionless Factor

Recent tests (March 2016) were realized to better understand the behavior of the SOLAR/SOLSPEC instrument. The scanning mechanism was maintained at a fixed position in order to measure the SSI evolution over time at a given

wavelength (210.2 nm). This test highlights that the instrument is unstable during short-time period (∼6% of variation). It was repeated several times (Figure 3), which shows the reversibility of the instrumental effect ($I_E(\lambda, t)$). SOLAR/SOLSPEC measurements during 20 minutes show SSI variations that are above the expected values during a solar cycle. The thermo-mechanical stability of the instrument is questionable and requires an opto-thermo-mechanical analysis. One can notice that during SOLAR/SOLSPEC switch-on, the signature of the signal is slightly different. Currently, we try to understand the link between the SOLAR/SOLSPEC UV photo-multiplier (UV PM) temperature and the measured signal.

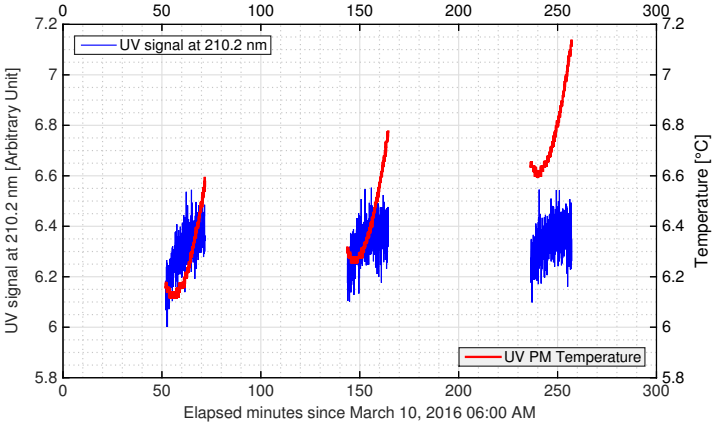

Figure 3. The red curve represents the UV PM temperature evolution during a calibration test. The SOLAR/SOLSPEC signal ($S_n(t)$ at 210.2 nm) evolves during a short time period (the blue curve). This instability effect should be corrected.

2.5. Irreversible Instrumental Effects Mainly Depicted by the $Deg(\lambda, t)$ Dimensionless Factor

Until April 2009, the degradation of the instrument ($Deg(\lambda, t)$) has been important (Figure 4) and was wavelength dependent. There is a dramatic aging due to the deuterium lamps use. From April 2009 to mid-2010, the degradation began to decrease. Since mid-2010, the SOLAR/SOLSPEC degradation follows a two-term exponential model where two degradation modes exist. The instrument is composed of several optical elements, which have different degradation time process. This law is demonstrated for different wavelengths of the instrument with different time responses. As a reminder, the instrument contains four lamps (nominal and spare) for checking the responsivity ($R(\lambda, t)$) of the 'UV' and 'VIS' spectrometers in order to correct the degradation. As explained in Section 2, the aging correction with the lamps is not trivial. This work is still in progress. Firstly, we can make the assumption that the degradation follows an exponential law to control the ability of SOLAR/SOLSPEC for measuring UV variability.

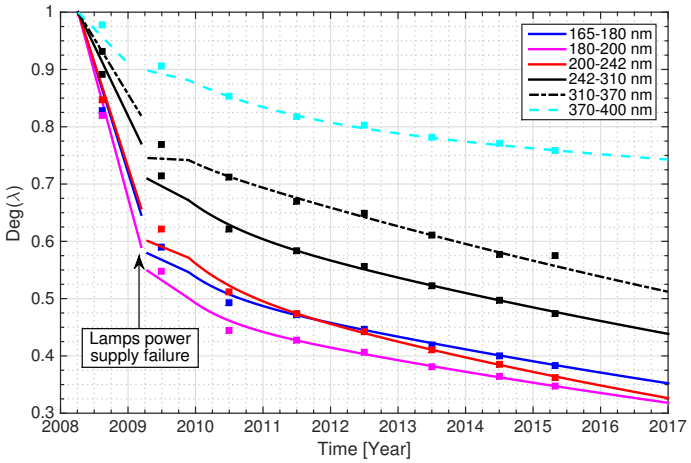

Figure 4. For different spectral bands, the evolution of the degradation during time is plotted. The square markers represent the annual mean measurements for each spectral bands.

2.6. SOLAR/SOLSPEC Main Temperatures Evolutions – $\alpha_T(\lambda, t)$ and $I_E(\lambda, t)$

Over time, the main shutter temperature of SOLAR/SOLSPEC increases (Figure 5, top), which highlights the degradation of the instrument thermal control. One can notice a temperature increase of $\sim 5^o$C from April 2008 to mid-2015. The instrument thermal heat sink facing the Sun uses a white paint, which degrades over time (increase of solar absorption). That is another level of degradation that impacts the temperature of the instrument and introduces temperature gradients. Figure 5 (bottom) displays the mean SOLAR/SOLSPEC temperatures (UV PM, main shutter, and centre plate) of the time series as a function of wavelength. As a reminder, the duration to record a solar spectrum is less than 17 minutes. Since the beginning of the mission, the measurement process is the same. Indeed, all gratings are rotating and scanning the three 'UV'–'VIS'–'IR' spectral ranges at the same time from short wavelengths toward higher.

The mean temperature of the UV photo-multiplier (UV PM) is close to 5^oC during each SSI measurement. During the absolute calibration at the PTB, the UV PM's temperature was close to 23^oC. Thus, the SSI as seen by SOLAR/SOLSPEC ($SSI_S(\lambda, t)$) requires a thermal correction ($\alpha_T(\lambda, t)$) of the UV PM temperature that is wavelength dependent. However, this thermal correction is weak and depends on the PM manufacturer data. One can notice that the temperature between the front face of the instrument (main shutter) and the central part (centre plate) is not the same. Moreover, they change significantly during the SSI measurements. There is $\sim 7.5^o$C of variation for the front face and $\sim 2.5^o$C of variation for the central part of the instrument. There is a thermal gradient on SOLAR/SOLSPEC between the front face and the central part, which is wavelength dependent. Thus, there is mechanical distortions on SOLAR/SOLSPEC due to thermal gradients that cause displacement of inter-

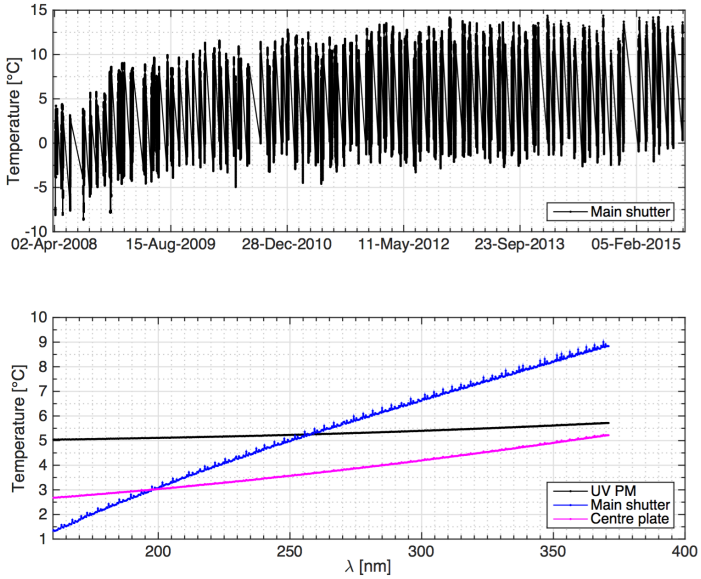

Figure 5. (top) Temperature evolution of SOLAR/SOLSPEC main shutter from April 2008 to mid-2015. (bottom) The Y-axis represents the mean temperatures (UV PM, main shutter, and SOLAR/SOLSPEC centre plate) from April 2008 to mid-2015 during SSI measurement with the 'UV' spectrometer at a given wavelength (X-axis).

mediate and exit slits. The understanding of this phenomenon is still under study and requires a correction to SOLAR/SOLSPEC data ($I_E(\lambda, t)$).

2.7. Wavelengths Shift Effect

As a reminder, SOLAR/SOLSPEC has a mechanism (gratings positioning) for directing the selected color to an exit slit. On SOLAR/SOLSPEC raw data, wavelengths shift were observed over time as shown in Figure 6 (top). This effect requires a correction of raw data, which follows a one-term exponential law (stability of the mechanism and its stepper motor that supports the gratings). After applying this correction, Equation 2 is applicable.

3. Results and Discussion

3.1. SOLAR/SOLSPEC Solar Irradiance from 165 to 400 nm (2008 Minimum)

Accurate determination of the solar irradiance from 165 to 400 nm is challenging. Calibration is an essential part of any space-based instrument. SOLAR/SOLSPEC response was precisely characterized (radiometric calibration, wavelength calibration, slit-function characterization, stray-light, field of view, *etc.*) during on-ground calibration phase (Bolsée, 2012). This step will allow us to have the initial values to determine the UV SSI variability.

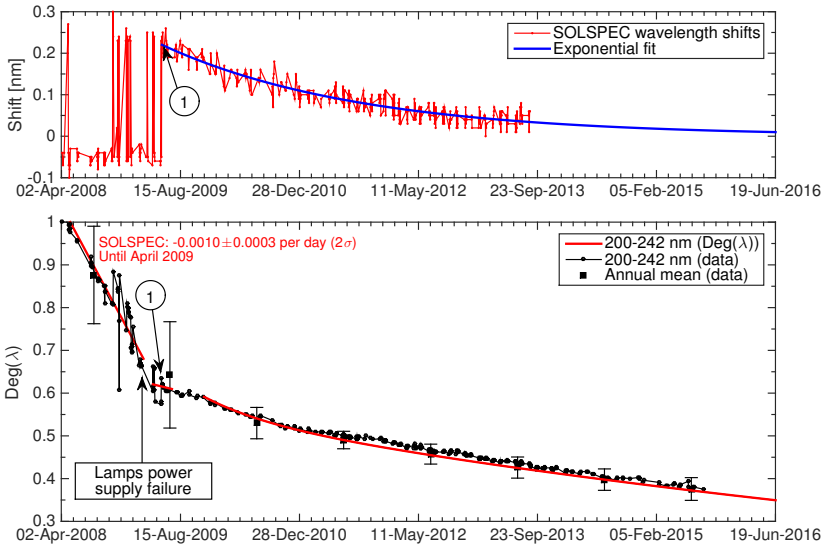

Figure 6. (top) SOLAR/SOLSPEC wavelengths shift. Marker 1 corresponds to a transition period. (bottom) Estimation of the degradation during time for the 200–242 nm band. A first linear fit corresponds to the degradation of SOLAR/SOLSPEC during the use of deuterium lamps (April 2008 to April 2009). A second fit corresponds to the transition period (transient outgassing period, wavelengths shift, *etc.*). A third exponential fit (Levenberg-Marquardt method) corresponds to SOLAR/SOLSPEC degradation from September 2009 to now. This fit is based on all points in the period 2009-2010 where solar activity is close to zero and on annual mean data. Uncertainty of the third exponential fit is ±0.0065 (1σ) on $Deg(\lambda, t)$ values.

The main challenge is to keep the ground-based characterization of the instrument during in space operations. Sun-observing instruments exposed to the space environment degrade due to the harsh space environment. SOLAR/SOLSPEC does not escape the rule (Figure 4). It is very important to monitor the degradation during the time of the mission and to have in-flight calibration for correcting the raw data. The SOLAR/SOLSPEC responsivity change is derived from comparison of the transmission of the second quartz plate (infrequently used), direct quartz-plate transmission measurements, and deuterium lamps data. The main correction is obtained from deuterium lamps. SOLAR/SOLSPEC used two deuterium lamps, which may have the same behavior in space. However, their rate of use during in-space calibrations are different inducing a different aging and therefore a different correction. Thus, the correction of SOLAR/SOLSPEC raw data by using the deuterium lamps is not obvious. From Figure 1, the degradation of the signal (200–242 nm) seen by the instrument with the D1 lamp is close to -0.11±0.01% per day ($2\,\sigma$). From Figure 6 (bottom), the degradation of the instrument (200–242 nm) is estimated at -0.10±0.03% per day. These results are consistent and facilitated by the fact that solar activity is close to zero during this period. However, the degradation of the signal (200–242 nm) seen by the instrument with the D2 lamp is more higher (-0.18±0.01% per day). By standardizing lamp operating time (D1t), the degradation of the signal (200–

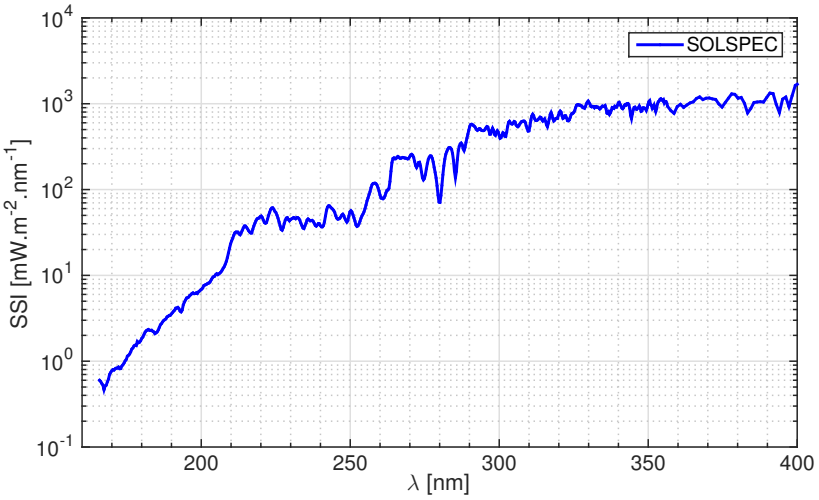

Figure 7. Solar irradiance from 165 to 400 nm as measured by SOLAR/SOLSPEC with the proposed method.

242 nm) seen by the instrument with the D1 lamp is close to that seen by the D2 lamp. The lamps have deteriorated as the instrument.
Another approach is to define a UV solar spectrum using the properties of Equation 2. The ideal case corresponds to a configuration where the instrument is not affected by the degradation ($Deg(\lambda, t)$=1) and by the instrumental effects ($I_E(\lambda, t)$=1). We emphasize that SOLAR/SOLSPEC consists of a subtractive three double-spectrometers. Instrumental effects tend to reduce the measured SSI. Thus, the SSI maximum values measured by SOLAR/SOLSPEC ($SSI_S(\lambda, t)$) from April 2008 to December 2008 correspond to the most probable SSI values of the real UV solar spectrum during the 2008 minimum. The red curve (Figure 2) is close to the most probable UV solar spectrum without temperature coefficient of the UV PM correction. Most of the SSI values used on this UV solar spectrum are derived from SOLAR/SOLSPEC spectra acquired from April 2008 to June 2008 (instrument BOL and quiet Sun). Figure 7 displays the UV solar spectrum using the thermal correction ($\alpha_T(\lambda, t)$) at the temperature associated with the wavelength measurement (Figure 5, bottom). Two SOLAR/SOLSPEC spectrometers ('UV' spectral band between 165.86 and 356.26 nm and 'VIS' spectral band between 356.50 and 400.42 nm) were used to obtain this UV solar spectrum (resolution and uncertainty optimization).

3.2. Definition of the SOLAR/SOLSPEC Analyzed Spectral Bands

To assess the SOLAR/SOLSPEC UV spectrum (Figure 7), comparisons are needed with reference spectra (ATLAS 3, WHI 2008) or model (SATIRE-S). In this article, we limited our study to a comparison with the SATIRE-S semi-empirical model. However, other solar models exist and could be compared.

Several spectral bands considered as important absorption bands of solar radiation (Brasseur and Solomon, 2005) were selected in order to compare different data sets (Table 1) and to improve the number of sample data to analyze (for the UV solar variability, see Section 3.5).

Table 1. Important absorption bands of solar radiation in the mesosphere, stratosphere, and troposphere.

$\Delta\lambda$ [nm]	Absorber	Principal location
165–200	O_2 Schumann–Runge bands	Thermosphere / Mesosphere
200–242	O_2 Herzberg continuum / O_3 Hartley band	Stratosphere
242–310	O_3 Hartley band	Stratosphere
310–400	O_3 Huggins band	Stratosphere / Troposphere

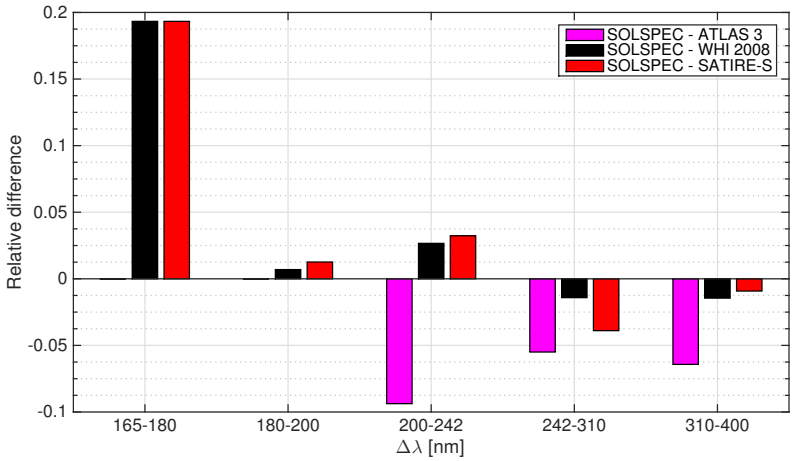

Figure 8. Relative differences between SOLAR/SOLSPEC and different reference spectra (ATLAS 3, WHI 2008) or model (SATIRE-S).

3.3. Differences between SOLAR/SOLSPEC and different Reference Spectra

Figure 8 displays the relative differences between SOLAR/SOLSPEC and different reference spectra (ATLAS 3, WHI 2008) or model (SATIRE-S). WHI 2008 solar spectrum was convolved to the SOLAR/SOLSPEC resolution. The SSI variability calculated from the SATIRE-S semi-empirical model is set on the WHI 2008 reference spectra (Yeo *et al.*, 2014) for some wavelength bands.
Figures 9 and 10 display SSI from 165 to 400 nm for SOLAR/SOLSPEC, ATLAS 3, WHI 2008, and SATIRE-S. Between 180 and 400 nm, difference between SOLAR/SOLSPEC and WHI 2008 or SATIRE-S is less than 5% while the difference between SOLAR/SOLSPEC and ATLAS 3 is greater than 10%. Data used in the ATLAS 3 spectrum suffered a 1.4% reduction (Thuillier *et al.*, 2003).

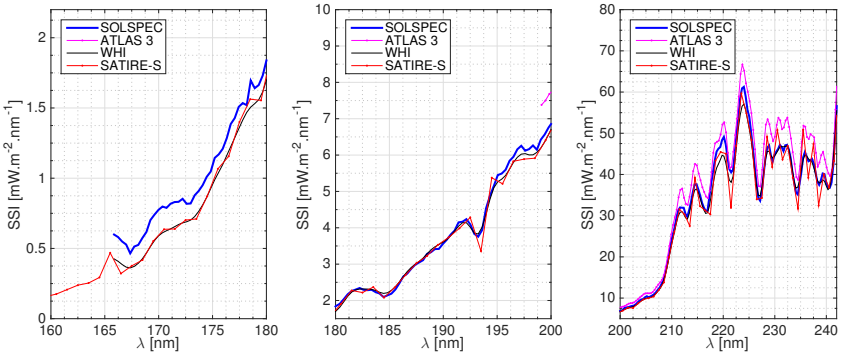

Figure 9. Solar irradiance for three spectral bands (165–180 nm, 180–200 nm and 200–242 nm) as seen by SOLAR/SOLSPEC, ATLAS 3, WHI 2008, and SATIRE-S.

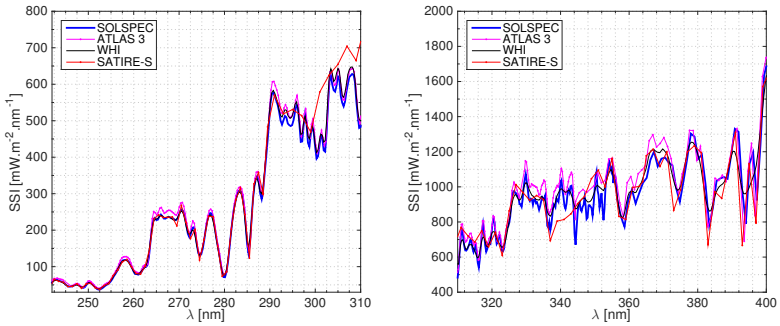

Figure 10. Solar irradiance for two spectral bands (242–310 nm and 310–400 nm) as seen by SOLAR/SOLSPEC, ATLAS 3, WHI 2008, and SATIRE-S.

ATLAS 3 was normalized with a standard value of the total solar irradiance (TSI) of 1367.7 W m^{-2}. Between 200 and 2400 nm, ATLAS 3 solar illumination is equal to 1315.7 W m^{-2} in agreement with a TSI of 1367.7 W m^{-2}. Today, the consensus absolute value of the TSI is close to 1361–1362 W m^{-2} (Kopp and Lean, 2011; Schmutz *et al.*, 2013; Meftah *et al.*, 2014b). It seems that the normalization of the ATLAS 3 spectrum is insufficient and could explain the greatest SSI values. Thus, the uncertainty analysis of UV and visible data obtained during the ATLAS 3 mission is questionable. Conversely, SOLAR/SOLSPEC with its uncertainty budget, the WHI 2008 solar spectrum, and the SATIRE-S solar spectrum were found in good agreement in the 180–400 nm spectral band. Between 165 and 180 nm, the differences between SOLAR/SOLSPEC and WHI 2008 or SATIRE-S are of ∼20%. In this spectral band, the agreement is not good. One can notice that the SOLAR/SOLSPEC SSI from 165 to 180 nm is greater than the WHI 2008 SSI or the SATIRE-S SSI in the same band. This may be due to a SOLAR/SOLSPEC ground-based calibration error and or the linearization of the UV signal at low wavelengths. However, we do not exclude that the WHI 2008 SSI is smaller in this spectral band and requires a correction. As a reminder, one can notice than SATIRE-S is wedged on the measurements made by WHI 2008.

3.4. Interest of the UV SSI Variability and Difficulty to Perform Measurements

Precise UV SSI variability measurements are required to quantify the top-down mechanism amplifying UV solar forcing on the climate despite the fact that the UV range (115.5 - 400 nm) represents only ∼7.7% of the TSI. The main uncertainty in the solar models concerns the wavelength range between 220 and 400 nm, where the magnitude of the variations differs by as much as a factor of three between models (Ermolli *et al.*, 2013). UV wavelengths can vary significantly during solar cycles. *SOLar STelar Irradiance Comparison Experiment* (SOLSTICE, 115–320 nm) and *Spectral Irradiance Monitor* (SIM, 300–2400 nm) (Harder *et al.*, 2005) measurements onboard the *Solar Radiation and Climate Experiment* (SORCE) space-based mission exhibit an unexpected behavior (Harder *et al.*, 2009). Currently there is insufficient observational evidence to validate the spectral variations observed by SOLSTICE and SIM. Haigh *et al.* (2010) have showed that such a spectral variability would lead to a significant change in the understanding of ozone evolution and atmospheric dynamics. The UV variability yielded by SIM and SOLSTICE indicates that the Sun can have substantially contributed to the observed trends of stratospheric ozone from 2004 to 2007. There is an ongoing discussion whether SOLSTICE and SIM did reveal a real solar behavior, or if its measurements were affected by uncorrected sensitivity drifts (Lean and DeLand, 2012). Overall, the comparison shows that the atmospheric changes simulated with the 3D chemistry-climate SOlar Climate Ozone Links (SOCOL) model driven by the SIM and SOLSTICE SSI are closest to the atmospheric measurements (Shapiro *et al.*, 2013). UV SSI variations measurements are questionable and new time series obtained by space-based instruments are of great interest.

3.5. SOLAR/SOLSPEC SSI Variations in Three Spectral Bands

SOLAR/SOLSPEC provides important UV SSI variations contribution monitoring during Solar Cycle 24. We limit this analysis at three spectral bands (165–180 nm, 180–200 nm, and 200–242 nm) due to SOLAR/SOLSPEC instrument effects (Section 2). Equation 3 allows to determine the SOLAR/SOLSPEC SSI evolution over time in three spectral bands.

$$SSI_{\Delta\lambda}(t_d) = \frac{1}{\Delta\lambda} \int_{\lambda_1}^{\lambda_2} SSI_R(\lambda, t_d)\, d\lambda\,, \tag{3}$$

where $SSI_{\Delta\lambda}(t_d)$ is the mean SOLAR/SOLSPEC SSI value in the desired spectral band ($\Delta\lambda$) over time, and t_d corresponds to a daily mean time.

With this method, we have collected quantitative data in a spectral band to carry out statistical analysis of the evolution of the mean value ($SSI_{\Delta\lambda}(t_d)$). Figure 11 displays the UV SSI variations as seen by the SOLAR/SOLSPEC instrument during Solar Cycle 24. Similarly, we plotted the SATIRE-S SSI variations in three spectral bands (165–180 nm, 180–200 nm, and 200–242 nm). Figure 12 displays the direct comparison between the ratio SOLAR/SOLSPEC over SATIRE-S for the period between April 2010 and August 2015. The ratio

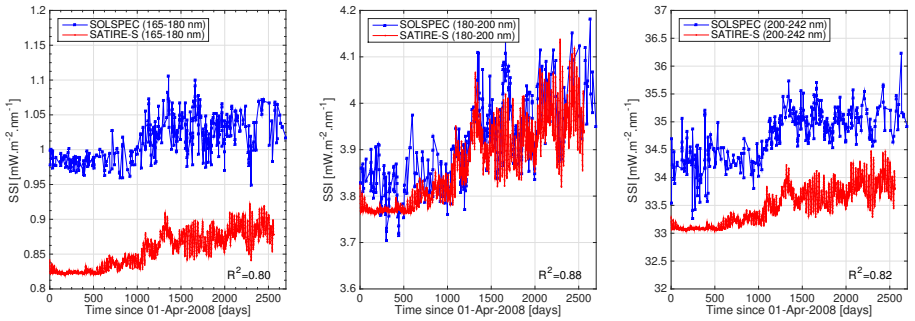

Figure 11. UV SSI variability in three spectral bands (165–180, 180–200, and 200–242 nm) during Solar Cycle 24. The blue curves with dots correspond to the measurement made by SOLAR/SOLSPEC. The red curves represent the values obtained with the SATIRE-S model. R^2 is the Pearson's linear correlation coefficient between SOLAR/SOLSPEC and SATIRE-S data.

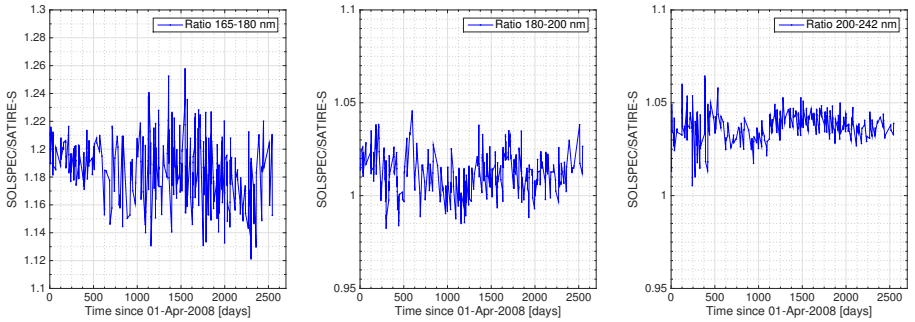

Figure 12. Data comparison between SOLAR/SOLSPEC and SATIRE-S in three spectral bands (165–180, 180–200, and 200–242 nm).

indicates that both data sets agree within ±5% for the peak-to-peak values. The absolute differences between SOLAR/SOLSPEC and SATIRE-S time series depend on the initial SOLAR/SOLSPEC values (see solar spectrum defined in Figure 7). Absolute deviations correspond to those given in Table 9. In the different spectral bands, the Pearson correlation coefficients (R^2) between SOLAR/SOLSPEC and SATIRE-S time series are higher than 0.8 that might indicate very strong relationship during same time operation. In the 180–200 nm spectral band, R^2 between SOLAR/SOLSPEC and SATIRE-S time series is close to 0.88. In this spectral band, the similarities are the best between SOLAR/SOLSPEC and SATIRE-S (UV variability and absolute value). It is also in this band than the instrument is the most stable (temperature gradient between the front part (main shutter) and the centre plate is close to zero as seen in Figure 5). These comparisons were not made with the SORCE instruments because there is a data gap in 2013. Indeed, all SORCE instruments ceased operations from July 30, 2013 to December 22, 2013 due to an anomaly of the satellite (battery degradation).

Table 2. Maximum UV SSI variations from 2008 to 2015 for SOLAR/SOLSPEC (with statistical uncertainty), SATIRE-S, and SORCE/SOLSTICE.

$\Delta\lambda$ [nm]	SOLAR/SOLSPEC	SATIRE-S	SORCE/SOLSTICE
Lyman-α (comparison)	–	–	∼28%
165–180	∼7.0±2.0% (1σ)	∼6.7%	∼8.3%
180–200	∼6.9±2.5% (1σ)	∼5.4%	∼8.2%
200–242	∼3.5±1.7% (1σ)	∼2.1%	∼3.1%

For each data set, we compute the difference between the minimum and the maximum of the UV SSI variations from 2008 to 2015 (Table 2). Each data set was filtered with a 51.9-days moving mean. In the 165–180 nm spectral band, the results are close for each data set. In the 180–200 nm spectral band, SOLAR/SOLSPEC maximum UV SSI variation is between SATIRE-S and SORCE/SOLSTICE. In the 200-242 nm spectral band, SOLAR/SOLSPEC maximum UV SSI is slightly higher than SORCE/SOLSTICE maximum variation. However, there is a significant difference with SATIRE-S maximum SSI variation from 2008 to 2015. This difference can be explained by an instrumental effect (see Sections 2.4 to 2.7) and by the use of a wider spectral band of analysis ($\Delta\lambda$=42 nm).

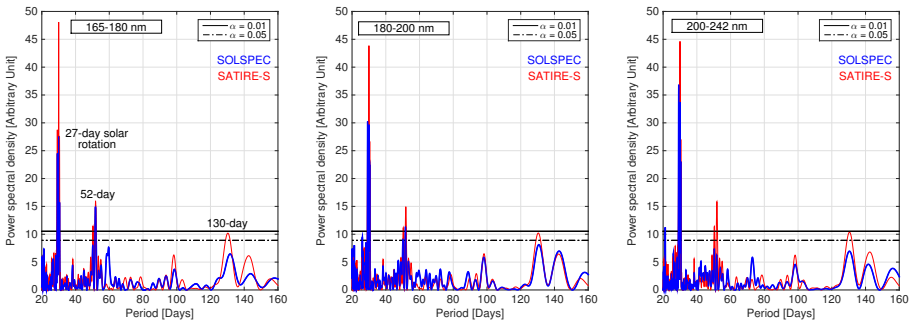

Figure 13. Lomb-Scargle periodogram for unevenly sampled time series (SOLAR/SOLSPEC) in three spectral bands (165–180, 180–200, and 200–242 nm) from 2008 to 2015. The blue curves correspond to the SOLAR/SOLSPEC periodogram. The red curves correspond to the SATIRE-S periodogram. α correspond to the statistical significance levels (0.01 corresponds to 99% significance level).

For a better comparison of the results, a spectral analysis for each data set was carried out. We took the same time of observations as those made by SOLAR/SOLSPEC from 2008 to 2015. Figure 13 displays the Lomb-Scargle periodograms of two time-series (daily mean), which show the link between SOLAR/SOLSPEC and the SATIRE-S semi-empirical model. Similar solar periodicities were highlighted (∼27, ∼52, and ∼130 days). One can notice a SOLAR/SOLSPEC solar periodicity ∼60 days (not significant) in the 165-180 nm spectral band. This period was also observed with the Sun Ecartometry Sensor

(SES) of the *Picard* mission at 782 nm, which is also observed in *Picard* solar radius data and sunspot number data.

4. Conclusions

SOLAR/SOLSPEC provides SSI data since April 2008 without discontinuity. Operations were very well managed since the beginning of the mission, where there is a repeatability of the observation sequences. The instrument degradation process corresponds to a two-term exponential model. A method was developed to determine the SOLAR/SOLSPEC SSI evolution during Solar Cycle 24. SOLAR/SOLSPEC provides preliminary new time series of the UV solar spectral irradiance from 2008 to 2015, which are consistent with the SATIRE-S semi-empirical model. During this period, the peak-to-peak UV variation (data with 51.9-days moving mean) is close to ∼7% in the 165-200 nm spectral band from 2008 to 2015. In the 200-242 nm spectral band, the peak-to-peak UV variation is close to ∼3.5%. This last result has to be consolidated with a more in-depth analysis. Indeed, this result is higher than that obtained from the SATIRE-S semi-empirical model and close to the SORCE/SOLSTICE observations. SOLAR/SOLSPEC can be assumed valid for short-term variations. On longer timescales, SOLAR/SOLSPEC stability is lower and requires a better characterization of instrument effects and degradation. Finally, we plan to use the helium hollow cathode lamp to correct the data. However, we need to do a ground test to characterize the aging of the lamp.

Acknowledgements The SOLAR/SOLSPEC investigation is supported by the Royal Belgian Institute for Space Aeronomy, by the Centre National d'Etudes Spatiales (CNES, France), by the Bundesministerium für Forschung und Technologie (Germany), and by the Centre National de la Recherche Scientifique (CNRS, France). The authors would like to thank the Laboratory for Atmospheric and Space Physics (LASP, United States) for providing the SORCE data and the Max Planck Institute for Solar System Research (Germany) for providing the SATIRE-S data. The authors gratefully acknowledge the anonymous reviewer for carefully reading the manuscript and providing constructive comments that have led to an improved paper.

Disclosure of Potential Conflicts of Interest: The authors declare that they have no conflicts of interest.

Appendix

A. Spectral Irradiance of the Sun ($\mathbf{mW\,m^{-2}\,nm^{-1}}$) from 165 to 400 nm

λ [nm]	SSI	λ [nm]	SSI	λ [nm]	SSI	λ [nm]	SSI
165.857	0.599	222.239	45.192	274.889	134.376	323.807	690.104
166.233	0.581	222.590	50.064	275.216	149.335	324.111	743.844
166.608	0.549	222.942	54.262	275.544	173.970	324.414	771.529
166.984	0.528	223.293	58.708	275.871	200.941	324.717	773.209
167.359	0.465	223.644	60.904	276.198	225.442	325.020	793.983
167.734	0.514	223.995	61.263	276.525	238.941	325.323	830.073
168.109	0.525	224.346	58.980	276.852	246.952	325.626	900.620
168.484	0.574	224.697	55.683	277.179	245.685	325.929	959.877
168.858	0.616	225.048	54.019	277.505	232.580	326.231	973.656
169.233	0.702	225.398	50.357	277.831	210.076	326.533	976.791
169.607	0.740	225.748	46.485	278.158	181.381	326.835	961.741
169.981	0.774	226.098	42.056	278.484	158.748	327.137	962.805
170.355	0.798	226.448	37.879	278.809	136.648	327.439	944.016
170.729	0.789	226.798	34.329	279.135	110.741	327.741	939.080
171.103	0.818	227.148	33.629	279.461	86.011	328.042	900.976
171.476	0.830	227.497	35.963	279.786	71.505	328.343	900.134
171.850	0.832	227.846	40.246	280.111	71.024	328.645	886.482
172.223	0.853	228.195	44.061	280.436	85.003	328.946	928.108
172.596	0.818	228.544	46.545	280.761	111.498	329.246	999.703
172.969	0.820	228.893	47.055	281.086	148.563	329.547	1041.406
173.342	0.878	229.242	44.662	281.411	189.079	329.848	1073.258
173.714	0.909	229.591	43.188	281.735	226.385	330.148	1030.379
174.087	0.951	229.939	44.704	282.059	257.847	330.448	986.555
174.459	1.010	230.287	45.541	282.384	276.734	330.748	930.130
174.831	1.047	230.635	46.172	282.708	294.397	331.048	918.669
175.203	1.145	230.983	47.182	283.031	306.654	331.348	932.695
175.575	1.170	231.331	46.656	283.355	309.000	331.648	929.176
175.947	1.210	231.678	45.684	283.679	304.639	331.947	897.980
176.318	1.284	232.026	47.081	284.002	294.066	332.246	926.533
176.690	1.386	232.373	47.179	284.325	263.623	332.545	929.576
177.061	1.428	232.720	46.073	284.648	218.024	332.844	907.064
177.432	1.508	233.067	44.082	284.971	163.512	333.143	911.923
177.803	1.535	233.414	40.594	285.294	136.983	333.442	891.378
178.173	1.520	233.761	38.061	285.616	162.033	333.740	868.515
178.544	1.696	234.107	35.676	285.939	223.041	334.039	888.531
178.914	1.641	234.454	35.141	286.261	283.383	334.337	916.906
179.285	1.663	234.800	37.739	286.583	319.981	334.635	939.908
179.655	1.730	235.146	40.501	286.905	340.212	334.933	927.881
180.025	1.845	235.492	44.115	287.227	348.050	335.231	933.436
180.395	1.909	235.838	45.454	287.549	334.821	335.528	951.445
180.764	2.037	236.183	44.383	287.870	300.181	335.826	880.151
181.134	2.173	236.529	43.191	288.192	284.971	336.123	777.630
181.503	2.261	236.874	43.417	288.513	308.893	336.420	769.049
181.872	2.301	237.219	43.781	288.834	353.363	336.717	800.060
182.241	2.343	237.564	42.640	289.155	396.957	337.014	752.909
182.610	2.293	237.909	40.457	289.475	442.101	337.311	783.136
182.979	2.285	238.253	38.215	289.796	492.966	337.607	839.202
183.348	2.296	238.598	37.473	290.116	546.323	337.903	902.752
183.716	2.231	238.942	38.625	290.437	573.936	338.200	894.826
184.084	2.193	239.286	40.236	290.757	576.660	338.496	883.369
184.452	2.095	239.630	40.084	291.077	567.718	338.792	935.135
184.820	2.142	239.974	38.002	291.397	555.821	339.087	922.376
185.188	2.188	240.318	36.797	291.716	543.513	339.383	913.634
185.556	2.303	240.662	36.766	292.036	524.794	339.678	959.638
185.923	2.473	241.005	38.016	292.355	500.449	339.973	1025.538
186.291	2.660	241.348	42.228	292.674	489.369	340.269	1038.339
186.658	2.740	241.691	49.270	292.993	500.750	340.564	982.402
187.025	2.873	242.034	57.292	293.312	513.012	340.858	941.040
187.392	2.983	242.377	62.599	293.631	509.500	341.153	890.180
187.758	3.047	242.720	64.741	293.949	492.328	341.447	874.766
188.125	3.109	243.062	64.413	294.268	487.963	341.742	904.017

188.491	3.282	243.404	62.258	294.586	485.486	342.036	960.281
188.857	3.329	243.747	60.565	294.904	487.935	342.330	981.280
189.224	3.414	244.089	59.129	295.222	501.939	342.624	965.968
189.589	3.419	244.430	57.125	295.540	524.518	342.917	1003.732
189.955	3.554	244.772	54.411	295.857	542.201	343.211	1006.671
190.321	3.670	245.114	49.613	296.175	535.238	343.504	971.262
190.686	3.812	245.455	46.467	296.492	493.135	343.798	880.364
191.052	3.924	245.796	45.168	296.809	441.995	344.091	730.872
191.417	4.149	246.137	45.466	297.126	443.126	344.384	669.991
191.782	4.166	246.478	46.156	297.443	488.306	344.676	761.981
192.147	4.237	246.819	48.001	297.760	519.187	344.969	849.561
192.511	4.092	247.160	50.407	298.076	492.302	345.262	905.354
192.876	3.834	247.500	51.609	298.393	439.522	345.554	913.399
193.240	3.755	247.840	49.567	298.709	428.883	345.846	870.241
193.604	3.937	248.181	46.203	299.025	464.549	346.138	860.401
193.968	4.535	248.521	43.703	299.341	485.192	346.430	886.470
194.332	4.880	248.860	41.791	299.657	467.911	346.721	896.511
194.696	5.155	249.200	43.544	299.972	429.029	347.013	939.945
195.060	5.450	249.540	49.189	300.288	396.152	347.304	894.458
195.423	5.492	249.879	54.964	300.603	402.313	347.596	816.531
195.786	5.597	250.218	56.715	300.918	430.602	347.887	825.086
196.150	5.841	250.557	54.874	301.233	459.611	348.178	894.675
196.513	5.953	250.896	50.929	301.548	452.223	348.468	895.904
196.875	6.159	251.235	46.859	301.863	418.657	348.759	888.494
197.238	6.255	251.573	42.971	302.177	415.268	349.049	877.896
197.601	6.121	251.912	38.629	302.492	465.414	349.340	836.923
197.963	6.164	252.250	37.231	302.806	541.064	349.630	894.882
198.325	6.264	252.588	37.782	303.120	607.579	349.920	977.397
198.687	6.147	252.926	39.788	303.434	623.870	350.210	1057.687
199.049	6.423	253.264	42.668	303.748	599.245	350.499	1085.598
199.411	6.565	253.602	46.342	304.061	583.641	350.789	980.583
199.772	6.758	253.939	49.480	304.375	579.700	351.078	952.896
200.134	6.909	254.277	51.870	304.688	596.510	351.367	882.700
200.495	7.132	254.614	55.068	305.001	621.033	351.656	917.771
200.856	7.615	254.951	59.862	305.314	612.437	351.945	964.146
201.217	7.723	255.288	65.930	305.627	567.150	352.234	876.652
201.578	7.799	255.624	73.886	305.939	549.206	352.523	809.977
201.939	7.954	255.961	79.803	306.252	539.353	352.811	875.010
202.299	8.100	256.297	87.014	306.564	552.868	353.099	996.755
202.659	8.169	256.634	94.349	306.876	580.174	353.387	1055.727
203.020	8.462	256.970	105.232	307.188	600.808	353.675	1076.958
203.380	8.929	257.306	113.687	307.500	619.688	353.963	1127.047
203.740	9.379	257.642	117.444	307.812	623.848	354.251	1143.025
204.099	9.651	257.977	118.198	308.124	628.104	354.538	1116.110
204.459	9.751	258.313	118.723	308.435	626.125	354.826	1088.138
204.818	10.196	258.648	116.944	308.746	605.675	355.113	1114.213
205.177	10.450	258.983	112.572	309.057	552.326	355.400	1021.510
205.537	10.189	259.318	104.909	309.368	512.840	355.687	1064.785
205.895	10.414	259.653	96.427	309.679	480.267	355.973	1060.818
206.254	10.649	259.988	86.326	309.990	482.944	356.260	1006.610
206.613	10.967	260.322	79.657	310.300	547.232	356.500	931.963
206.971	11.434	260.657	79.617	310.610	642.743	357.578	832.407
207.330	12.065	260.991	78.133	310.921	721.065	358.656	772.831
207.688	12.579	261.325	79.881	311.231	753.544	359.733	926.022
208.046	13.450	261.659	84.373	311.541	726.554	360.810	984.591
208.404	14.521	261.993	91.940	311.850	671.960	361.887	905.480
208.761	16.096	262.326	98.175	312.160	640.507	362.964	966.117
209.119	18.226	262.660	98.893	312.469	636.576	364.040	1023.196
209.476	20.644	262.993	103.355	312.778	643.695	365.116	1050.862
209.834	23.266	263.326	124.006	313.087	658.184	366.191	1152.841
210.191	25.272	263.659	163.071	313.396	675.946	367.266	1201.418
210.548	27.025	263.992	205.728	313.705	698.203	368.341	1116.841
210.904	29.346	264.325	230.178	314.014	691.284	369.416	1160.355
211.261	31.294	264.657	233.984	314.322	650.239	370.490	1166.743
211.617	31.991	264.990	227.793	314.631	627.903	371.563	1137.563
211.974	31.937	265.322	228.852	314.939	644.596	372.637	1122.315
212.330	31.910	265.654	237.988	315.247	666.057	373.710	992.108
212.686	30.396	265.986	243.034	315.555	623.590	374.782	914.084
213.042	29.755	266.318	238.147	315.862	566.928	375.855	1032.612

213.397	31.406	266.649	231.847	316.170	539.636	376.927	1160.287
213.753	33.390	266.981	231.603	316.477	592.323	377.998	1303.037
214.108	35.766	267.312	234.407	316.784	667.594	379.069	1286.101
214.463	37.616	267.643	236.856	317.091	748.593	380.140	1158.626
214.818	37.616	267.974	234.994	317.398	790.203	381.211	1184.126
215.173	36.335	268.305	232.435	317.705	737.015	382.281	1014.179
215.528	34.850	268.636	232.674	318.012	668.032	383.351	780.206
215.883	33.138	268.966	229.507	318.318	630.149	384.420	879.851
216.237	31.971	269.297	227.379	318.624	645.055	385.490	1033.839
216.591	31.160	269.627	231.269	318.930	671.971	386.558	1047.708
216.946	31.196	269.957	241.787	319.236	677.292	387.627	1055.989
217.299	34.488	270.287	252.846	319.542	674.052	388.695	1045.526
217.653	37.727	270.616	257.143	319.848	732.872	389.763	1182.325
218.007	40.545	270.946	251.090	320.153	790.364	390.830	1330.439
218.360	43.420	271.275	236.991	320.459	820.567	391.897	1313.691
218.714	45.575	271.605	212.379	320.764	797.904	392.964	983.109
219.067	46.259	271.934	189.886	321.069	721.823	394.030	789.572
219.420	46.649	272.263	180.617	321.374	674.804	395.096	1131.682
219.773	48.363	272.592	190.125	321.679	685.815	396.162	1195.201
220.126	49.120	272.920	206.460	321.983	723.647	397.227	923.357
220.478	47.339	273.249	207.954	322.288	723.985	398.292	1238.139
220.831	44.101	273.577	188.891	322.592	684.011	399.357	1635.823
221.183	41.272	273.905	160.349	322.896	635.446	400.421	1718.332
221.535	40.507	274.233	136.890	323.200	632.407	–	–
221.887	41.139	274.561	129.725	323.504	646.485	–	–

References

Austin, J., Tourpali, K., Rozanov, E., Akiyoshi, H., Bekki, S., Bodeker, G., Brühl, C., Butchart, N., Chipperfield, M., Deushi, M., Fomichev, V.I., Giorgetta, M.A., Gray, L., Kodera, K., Lott, F., Manzini, E., Marsh, D., Matthes, K., Nagashima, T., Shibata, K., Stolarski, R.S., Struthers, H., Tian, W.: 2008, Coupled chemistry climate model simulations of the solar cycle in ozone and temperature. *Journal of Geophysical Research (Atmospheres)* **113**, D11306. doi:10.1029/2007JD009391.

BenMoussa, A., Gissot, S., Schühle, U., Del Zanna, G., Auchère, F., Mekaoui, S., Jones, A.R., Walton, D., Eyles, C.J., Thuillier, G., Seaton, D., Dammasch, I.E., Cessateur, G., Meftah, M., Andretta, V., Berghmans, D., Bewsher, D., Bolsée, D., Bradley, L., Brown, D.S., Chamberlin, P.C., Dewitte, S., Didkovsky, L.V., Dominique, M., Eparvier, F.G., Foujols, T., Gillotay, D., Giordanengo, B., Halain, J.P., Hock, R.A., Irbah, A., Jeppesen, C., Judge, D.L., Kretzschmar, M., McMullin, D.R., Nicula, B., Schmutz, W., Ucker, G., Wieman, S., Woodraska, D., Woods, T.N.: 2013, On-Orbit Degradation of Solar Instruments. *Solar Phys.* **288**, 389 – 434. doi:10.1007/s11207-013-0290-z.

Bolsée, D.: 2012, Métrologie de la spectrophotométrie solaire absolue: principes, mise en oeuvre et résultats ; instrument solspec à bord de la station spatiale internationale (unpublished doctoral dissertation). PhD thesis, Université libre de Bruxelles, École polytechnique de Bruxelles.

Bovensmann, H., Burrows, J.P., Buchwitz, M., Frerick, J., Noël, S., Rozanov, V.V., Chance, K.V., Goede, A.P.H.: 1999, SCIAMACHY: Mission Objectives and Measurement Modes. *J. Atmosph. Sci.* **56**, 127. doi:10.1175/1520-0469(1999)056<0127:SMOAMM>2.0.CO;2.

Brasseur, G.P., Solomon, S.: 2005, *Aeronomy of the Middle Atmosphere: Chemistry and Physics of the Stratosphere and Mesosphere*, 3rd.

Cebula, R.P., DeLand, M.T., Hilsenrath, E.: 1998, NOAA 11 solar backscattered ultraviolet, model 2 (SBUV/2) instrument solar spectral irradiance measurements in 1989-1994 1. Observations and long-term calibration. *J. Geophys. Res.* **103**, 16235 – 16250. doi:10.1029/98JD01205.

Cebula, R.P., Hilsenrath, E., Guenther, B.: 1989, Calibration of the Shuttle borne solar backscatter ultraviolet spectrometer. In: Palmer, J.M. (ed.) *Optical Radiation Measurements II, Proc. SPIE* **1109**, 205 – 218.

Cessateur, G., Schmutz, W., Wehrli, C., Gröbner, J., Haberreiter, M., Kretzschmar, M., Rozanov, E., Schöll, M., Shapiro, A., Thuillier, G., Egorova, T., Finsterle, W., Fox, N., Hochedez, J.-F., Koller, S., Meftah, M., Meindl, P., Nyeki, S., Pfiffner, D., Roth, H., Rouzé,

M., Spescha, M., Tagirov, R., Werner, L., Wyss, J.-U.: 2016, Solar irradiance observations with PREMOS filter radiometers on the PICARD mission: In-flight performance and data release. *Astron. Astrophys.* **588**, A126. doi:10.1051/0004-6361/201527577.

Ermolli, I., Matthes, K., Dudok de Wit, T., Krivova, N.A., Tourpali, K., Weber, M., Unruh, Y.C., Gray, L., Langematz, U., Pilewskie, P., Rozanov, E., Schmutz, W., Shapiro, A., Solanki, S.K., Woods, T.N.: 2013, Recent variability of the solar spectral irradiance and its impact on climate modelling. *Atm. Chem. Phys.* **13**, 3945. doi:10.5194/acp-13-3945-2013.

Haigh, J.D., Winning, A.R., Toumi, R., Harder, J.W.: 2010, An influence of solar spectral variations on radiative forcing of climate. *Nature* **467**, 696 – 699. doi:10.1038/nature09426.

Harder, J.W., Fontenla, J.M., Pilewskie, P., Richard, E.C., Woods, T.N.: 2009, Trends in solar spectral irradiance variability in the visible and infrared. *Geophys. Res. Lett.* **36**, 7801. doi:10.1029/2008GL036797.

Harder, J., Lawrence, G., Fontenla, J., Rottman, G., Woods, T.: 2005, The Spectral Irradiance Monitor: Scientific Requirements, Instrument Design, and Operation Modes. *Solar Phys.* **230**, 141. doi:10.1007/s11207-005-5007-5.

Hegglin, M.I., Gettelman, A., Hoor, P., Krichevsky, R., Manney, G.L., Pan, L.L., Son, S.-W., Stiller, G., Tilmes, S., Walker, K.A., Eyring, V., Shepherd, T.G., Waugh, D., Akiyoshi, H., AñEl, J.A., Austin, J., Baumgaertner, A., Bekki, S., Braesicke, P., Brühl, C., Butchart, N., Chipperfield, M., Dameris, M., Dhomse, S., Frith, S., Garny, H., Hardiman, S.C., JöCkel, P., Kinnison, D.E., Lamarque, J.F., Mancini, E., Michou, M., Morgenstern, O., Nakamura, T., Olivié, D., Pawson, S., Pitari, G., Plummer, D.A., Pyle, J.A., Rozanov, E., Scinocca, J.F., Shibata, K., Smale, D., TeyssèDre, H., Tian, W., Yamashita, Y.: 2010, Multimodel assessment of the upper troposphere and lower stratosphere: Extratropics. *Journal of Geophysical Research (Atmospheres)* **115**, D00M09. doi:10.1029/2010JD013884.

Kopp, G., Lean, J.L.: 2011, A new, lower value of total solar irradiance: Evidence and climate significance. *Geophys. Res. Lett.* **38**, 1706. doi:10.1029/2010GL045777.

Labs, D., Neckel, H.: 1968, The Radiation of the Solar Photosphere from 2000 Å to 100 μm. *Zeitschrift für Astrophysik* **69**, 1.

Lean, J.L., DeLand, M.T.: 2012, How Does the Sun's Spectrum Vary? *Journal of Climate* **25**, 2555 – 2560. doi:10.1175/JCLI-D-11-00571.1.

Meftah, M., Hochedez, J.-F., Irbah, A., Hauchecorne, A., Boumier, P., Corbard, T., Turck-Chièze, S., Abbaki, S., Assus, P., Bertran, E., Bourget, P., Buisson, F., Chaigneau, M., Damé, L., Djafer, D., Dufour, C., Etcheto, P., Ferrero, P., Hersé, M., Marcovici, J.-P., Meissonnier, M., Morand, F., Poiet, G., Prado, J.-Y., Renaud, C., Rouanet, N., Rouzé, M., Salabert, D., Vieau, A.-J.: 2014a, Picard SODISM, a Space Telescope to Study the Sun from the Middle Ultraviolet to the Near Infrared. *Solar Phys.* **289**, 1043. doi:10.1007/s11207-013-0373-x.

Meftah, M., Dewitte, S., Irbah, A., Chevalier, A., Conscience, C., Crommelynck, D., Janssen, E., Mekaoui, S.: 2014b, SOVAP/ Picard, a Spaceborne Radiometer to Measure the Total Solar Irradiance. *Solar Phys.* **289**, 1885 – 1899. doi:10.1007/s11207-013-0443-0.

Neckel, H., Labs, D.: 1981, Improved data of solar spectral irradiance from 0.33 to 1.25 microns. *Solar Phys.* **74**, 231 – 249. doi:10.1007/BF00151293.

Neckel, H., Labs, D.: 1984, The solar radiation between 3300 and 12500 A. *Solar Phys.* **90**, 205 – 258. doi:10.1007/BF00173953.

Oman, L.D., Plummer, D.A., Waugh, D.W., Austin, J., Scinocca, J.F., Douglass, A.R., Salawitch, R.J., Canty, T., Akiyoshi, H., Bekki, S., Braesicke, P., Butchart, N., Chipperfield, M.P., Cugnet, D., Dhomse, S., Eyring, V., Frith, S., Hardiman, S.C., Kinnison, D.E., Lamarque, J.-F., Mancini, E., Marchand, M., Michou, M., Morgenstern, O., Nakamura, T., Nielsen, J.E., Olivié, D., Pitari, G., Pyle, J., Rozanov, E., Shepherd, T.G., Shibata, K., Stolarski, R.S., TeyssèDre, H., Tian, W., Yamashita, Y., Ziemke, J.R.: 2010, Multimodel assessment of the factors driving stratospheric ozone evolution over the 21st century. *Journal of Geophysical Research (Atmospheres)* **115**, D24306. doi:10.1029/2010JD014362.

Pagaran, J., Weber, M., Burrows, J.: 2009, Solar Variability from 240 to 1750 nm in Terms of Faculae Brightening and Sunspot Darkening from SCIAMACHY. *Astrophys. J.* **700**, 1884. doi:10.1088/0004-637X/700/2/1884.

Pagaran, J., Harder, J.W., Weber, M., Floyd, L.E., Burrows, J.P.: 2011, Intercomparison of SCIAMACHY and SIM vis-IR irradiance over several solar rotational timescales. *Astron. Astrophys.* **528**, A67. doi:10.1051/0004-6361/201015632.

Schmutz, W., Fehlmann, A., Finsterle, W., Kopp, G., Thuillier, G.: 2013, Total solar irradiance measurements with PREMOS/PICARD. In: *American Institute of Physics*

Conference Series, *American Institute of Physics Conference Series* **1531**, 624 – 627. doi:10.1063/1.4804847.

Shapiro, A.V., Rozanov, E.V., Shapiro, A.I., Egorova, T.A., Harder, J., Weber, M., Smith, A.K., Schmutz, W., Peter, T.: 2013, The role of the solar irradiance variability in the evolution of the middle atmosphere during 2004-2009. *Journal of Geophysical Research (Atmospheres)* **118**, 3781 – 3793. doi:10.1002/jgrd.50208.

Strahan, S.E., Douglass, A.R., Stolarski, R.S., Akiyoshi, H., Bekki, S., Braesicke, P., Butchart, N., Chipperfield, M.P., Cugnet, D., Dhomse, S., Frith, S.M., Gettelman, A., Hardiman, S.C., Kinnison, D.E., Lamarque, J.-F., Mancini, E., Marchand, M., Michou, M., Morgenstern, O., Nakamura, T., Olivié, D., Pawson, S., Pitari, G., Plummer, D.A., Pyle, J.A., Scinocca, J.F., Shepherd, T.G., Shibata, K., Smale, D., TeyssèDre, H., Tian, W., Yamashita, Y.: 2011, Using transport diagnostics to understand chemistry climate model ozone simulations. *Journal of Geophysical Research (Atmospheres)* **116**, D17302. doi:10.1029/2010JD015360.

Sukhodolov, T., Rozanov, E., Ball, W.T., Bais, A., Tourpali, K., Shapiro, A.I., Telford, P., Smyshlyaev, S., Fomin, B., Sander, R., Bossay, S., Bekki, S., Marchand, M., Chipperfield, M.P., Dhomse, S., Haigh, J.D., Peter, T., Schmutz, W.: 2016, Evaluation of simulated photolysis rates and their response to solar irradiance variability. *Journal of Geophysical Research: Atmospheres*, n/a – n/a. 2015JD024277. doi:10.1002/2015JD024277. http://dx.doi.org/10.1002/2015JD024277.

Thuillier, G., Hersé, M., Labs, D., Foujols, T., Peetermans, W., Gillotay, D., Simon, P.C., Mandel, H.: 2003, The Solar Spectral Irradiance from 200 to 2400 nm as Measured by the SOLSPEC Spectrometer from the Atlas and Eureca Missions. *Solar Phys.* **214**, 1. doi:10.1023/A:1024048429145.

Thuillier, G., Foujols, T., Bolsée, D., Gillotay, D., Hersé, M., Peetermans, W., Decuyper, W., Mandel, H., Sperfeld, P., Pape, S., Taubert, D.R., Hartmann, J.: 2009, SOLAR/SOLSPEC: Scientific Objectives, Instrument Performance and Its Absolute Calibration Using a Blackbody as Primary Standard Source. *Solar Phys.* **257**, 185. doi:10.1007/s11207-009-9361-6.

von Hobe, M., Bekki, S., Borrmann, S., Cairo, F., D'Amato, F., Di Donfrancesco, G., Dörnbrack, A., Ebersoldt, A., Ebert, M., Emde, C., Engel, I., Ern, M., Frey, W., Genco, S., Griessbach, S., Grooß, J.-U., Gulde, T., Günther, G., Hösen, E., Hoffmann, L., Homonnai, V., Hoyle, C.R., Isaksen, I.S.A., Jackson, D.R., Jánosi, I.M., Jones, R.L., Kandler, K., Kalicinsky, C., Keil, A., Khaykin, S.M., Khosrawi, F., Kivi, R., Kuttippurath, J., Laube, J.C., Lefèvre, F., Lehmann, R., Ludmann, S., Luo, B.P., Marchand, M., Meyer, J., Mitev, V., Molleker, S., Müller, R., Oelhaf, H., Olschewski, F., Orsolini, Y., Peter, T., Pfeilsticker, K., Piesch, C., Pitts, M.C., Poole, L.R., Pope, F.D., Ravegnani, F., Rex, M., Riese, M., Röckmann, T., Rognerud, B., Roiger, A., Rolf, C., Santee, M.L., Scheibe, M., Schiller, C., Schlager, H., Siciliani de Cumis, M., Sitnikov, N., Søvde, O.A., Spang, R., Spelten, N., Stordal, F., Sumińska-Ebersoldt, O., Ulanovski, A., Ungermann, J., Viciani, S., Volk, C.M., vom Scheidt, M., von der Gathen, P., Walker, K., Wegner, T., Weigel, R., Weinbruch, S., Wetzel, G., Wienhold, F.G., Wohltmann, I., Woiwode, W., Young, I.A.K., Yushkov, V., Zobrist, B., Stroh, F.: 2013, Reconciliation of essential process parameters for an enhanced predictability of Arctic stratospheric ozone loss and its climate interactions (RECONCILE): activities and results. *Atmospheric Chemistry & Physics* **13**, 9233 – 9268. doi:10.5194/acp-13-9233-2013.

Woods, T.N., Chamberlin, P.C., Harder, J.W., Hock, R.A., Snow, M., Eparvier, F.G., Fontenla, J., McClintock, W.E., Richard, E.C.: 2009, Solar Irradiance Reference Spectra (SIRS) for the 2008 Whole Heliosphere Interval (WHI). *Geophys. Res. Lett.* **36**, L01101. doi:10.1029/2008GL036373.

Yeo, K.L., Krivova, N.A., Solanki, S.K., Glassmeier, K.H.: 2014, Reconstruction of total and spectral solar irradiance from 1974 to 2013 based on KPVT, SoHO/MDI, and SDO/HMI observations. *Astron. Astrophys.* **570**, A85. doi:10.1051/0004-6361/201423628.